Achievable Rate of Multiuser Scheduling in RIS-based Massive MIMO Systems

Cheonyong Kim¹, Minchae Jung², and Walid Saad¹

¹Wireless@VT, Bradley Department of Electrical and Computer Engineering, Virginia Tech, VA, USA Emails: {cheokim, walids}@vt.edu

²Department of Electronics and Information Engineering, Sejong University, Seoul, Republic of Korea Email: mcjung@sejong.ac.kr

Abstract—In this paper, the achievable sum rate of multiuser scheduling in reconfigurable intelligent surface (RIS)-based massive multiple-input multiple-output systems is investigated. Using asymptotic analysis under the generic condition of large numbers of base station antennas, RISs, and users, the RIS-based sum rate is proven to follow a Gaussian distribution. In addition, based on the characteristics of Gaussian distribution, the conditions for the occurrence of the channel hardening phenomenon and achievable scheduling gain are derived as a function of the number of RISs and users. Numerical results show that the derived RIS-based sum rate and the Monte Carlo simulation results are in close agreement as well as that the proposed achievable sum rate constitutes a meaningful bound to verify the performance of various multiuser scheduling algorithms.

Index Terms—Reconfigurable intelligent surface (RIS), achievable sum rate, user scheduling.

I. Introduction

The demand for massive connectivity and high data traffic in wireless communication systems has been growing exponentially in recent years, mainly driven by the increasing number of wireless devices and the appearance of new applications such as the Internet-of-things (IoT) [1]. For supporting the increasing number of devices and very high data traffic, many technologies have been proposed ranging from massive multiple-input multiple-output (MIMO) and millimeter-wave (mmWave) technologies to the use of various spectrum coexistence techniques. These technologies provide significant achievable rate gains but lead to additional power and hardware costs thereby restricting their overall efficiency.

Recently, reconfigurable intelligent surfaces (RISs) [2] have emerged as a promising solution for providing a high data rate without additional overhead at the transmitter. An RIS is made of low-cost and passive reflecting elements, each of which can manipulate the incident electromagnetic (EM) wave from the base station (BS) in terms of frequency, amplitude, and phase. The manipulated EM wave at an RIS is reflected towards destined user equipment (UE) so that a dedicated link is created between the BS and the UE. It is envisaged that future man-made structures (e.g., buildings, walls, roads, etc.) to be electromagnetically active [3] thereby acting as ubiquitous RISs providing extensive wireless connectivity.

This work was supported in part by the Basic Science Research Program through the National Research Foundation of Korea (NRF) funded by the Ministry of Education under Grant NRF-2021R1C1C1012950 and in part by the U.S. National Science Foundation under Grant CNS-2030215.

In the past few years, there has been significant interest in the design and deployment of RISs for enhanced wireless connectivity [4]–[9]. In [4], the authors formulated an optimization problem whose goal is to maximize the achievable rate of an RIS-based MIMO systems. The work in [5] addressed a joint optimization problem whose goal is to design the passive beamforming and the power allocation with the goal of maximizing energy efficiency. In [6], RISs are exploited to maximize energy efficiency in device-to-device communication network. The authors in [7] considered the massive access for IoT devices in RIS-based wireless systems. In [8], the authors developed a new approach to optimize RIS configuration in mmWave-based IoT systems using the federated learning. In [9], the authors analyzed the asymptotic achievable sum rate of RIS-based systems, and designed modulation and resource allocation schemes for enhancing the achievable sum rate. However, these prior works mainly focused on the ergodic sum rate, which results from the channel hardening effect [10] without considering the impact of a large number of RISs and UEs. For instance, the works in [4] and [5] formulated their maximization problems for an RIS and a UE whereas the works in [6]-[9] considered a given number of RISs and UEs without considering multiuser diversity. Given a large number of RISs and UEs, it is necessary to analyze the RIS-based multiuser diversity and the achievable scheduling gain.

The main contribution of this paper is, thus, an analysis of the achievable sum rate of multiuser scheduling in RIS-based massive MIMO systems consisting of a number of RISs and UEs. In this system, the achievable sum rate is defined by the maximum performance obtained by the optimal RIS-UE associations and multiuser scheduling under given massive connectivity to a large number of UEs using RISs. For this setting, we analyze the achievable improvement and the performance upper bound of a RIS-based system. In addition, we analyze the conditions for the occurrence of the channel hardening effect. In summary, our key contributions include:

Instead of using a computationally-prohibitive exhaustive search approach as done in [11], we derive the achievable sum rate of RIS-based MIMO systems through asymptotic analysis. Specifically, we prove that the RIS-based sum rate follows an independent and identically distributed (i.i.d.) Gaussian distribution whose characteristics allow us to obtain the achievable scheduling gain.

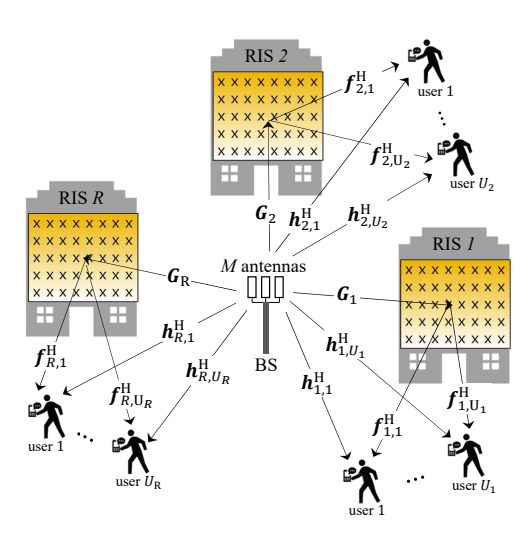


Fig. 1. System model of the RIS-based massive MIMO network consisting of RISs and users.

 We focus on the multiuser scheduling gain resulting from simultaneously scheduled multiple users. From the analysis of the achievable scheduling gain, we evaluate and characterize the channel hardening effect in multiuser RIS-assisted massive MIMO systems.

The rest of this paper is organized as follows. Section II describes the system model. Section III presents the analysis on the distribution of the RIS-based sum rate. Section IV presents the analysis on the RIS-based sum rate including achievable scheduling gain. Simulation results are provided in Section V and Section VI concludes this paper.

Notation: Throughout this paper, boldface upper- and lowercase symbols represent matrices and vectors respectively. The Hermitian transpose and Moor-Penrose pseudo inverse operators are denoted by $(\cdot)^H$ and $(\cdot)^\dagger$ respectively. The Frobenius norm is denoted by $\|\cdot\|_F$. $E[\cdot]$ and $Var[\cdot]$ denote expectation and variance operators, respectively.

II. SYSTEM MODEL

As shown in Fig. 1, we consider a single BS MIMO system that consists of U UEs and R RISs each of which has N reflecting elements. An RIS r is connected to $U_r \geq 1$ UEs so that $\sum_{r=1}^R U_r = U \geq R$. The BS is equipped with M antennas and serves K UEs (i.e., $K \leq U$ and $K \leq M$) at each resource block based on an orthogonal frequency-division multiple-access scheme. We consider a large M in the massive MIMO scenario. In addition, considering a very larger number of wireless devices and RISs, we assume that U and R are also very large, i.e., $U \geq R = M^c \gg K$, where c is considered to be a constant, to simplify the analysis.

Then, the received signal at UE u connected to RIS r will be given by:

$$y_{r,u} = \boldsymbol{h}_{r,u}^{\mathrm{H}} \boldsymbol{w}_{r,u} s_{r,u} + \boldsymbol{f}_{r,u}^{\mathrm{H}} \boldsymbol{\Phi}_{r} \boldsymbol{G}_{r} \boldsymbol{w}_{r,u} s_{r,u} + n_{r,u}, \quad (1)$$

where $h_{r,u} \in \mathbb{C}^{M \times 1}$, $G_r \in \mathbb{C}^{N \times M}$, $f_{r,u} \in \mathbb{C}^{N \times 1}$ are, respectively, the fading channels between the BS and UE u, between the BS and RIS r, and between the RIS and UE.

 $\Phi_r \in \mathbb{C}^{N \times N}$ is a matrix for passive beamforming including reflected amplitudes and phases by N reflecting elements. In a practical RIS-assisted network, RISs are installed at fixed locations whereas UEs are randomly deployed. Therefore, G_r is assumed to have a line of sight (LoS) channel whereas $h_{r,u}^H$ and $f_{r,u}^H$ are assumed to have a Rayleigh fading channel. Each element $(G_r)_{m,n}$ of G_r is given by $\exp\left(\frac{-j2\pi d_{m,r,n}}{\lambda}\right)$ where λ is the wavelength and $d_{m,r,n}$ is the distance between the mth antenna of the BS and the n th element of RIS r. The effective channel at UE r,u will be:

$$\boldsymbol{h}_{\text{eff},r,u}^{\text{H}} = \boldsymbol{h}_{r,u}^{\text{H}} + \boldsymbol{f}_{r,u}^{\text{H}} \boldsymbol{\Phi}_r \boldsymbol{G}_r = \boldsymbol{h}_{r,u}^{\text{H}} + \sqrt{N} \boldsymbol{z}_{r,u} \boldsymbol{R}_r^{1/2},$$
 (2)

where $\mathbf{z}_{r,u} \sim \mathcal{CN}(0, \mathbf{I}_M)$ and \mathbf{R}_r is a correlation matrix defined as $\frac{1}{N} \mathbf{G}_r^{\mathrm{H}} \mathbf{G}_r$ as proved in [12] and [13]. The aggregate downlink channel for the selected K UEs is defined as $\mathbf{H} = \left[\mathbf{h}_{\mathrm{eff},1}^{\mathrm{H}}, \cdots, \mathbf{h}_{\mathrm{eff},K}^{\mathrm{H}}\right]^{\mathrm{T}}$. We assume that the channel state information at transmitter (CSIT) of the aggregate downlink channel (i.e., \mathbf{H}) is perfectly known at the BS so that we can exploit zero-forcing beamforming (ZFBF). The assumption of having perfect knowledge of CSIT is idealistic but it allows us to derive the theoretical upper bound of the sum rate of an RIS-based system.

In a ZFBF-based multiuser MIMO system, maximum performance can be achieved by selecting user channels that are orthogonal [11]. Meanwhile, the RIS-based sum rate might experience a loss due to channel correlation since the UEs connected to the same RIS are highly correlated [12]. Therefore, to achieve the maximum RIS-based sum rate of K-user scheduling, the BS should select K RISs each of which is associated with one UE. Consequently, we consider selecting independent K RIS-UE pairs from $\{1,\cdots,R\}$ with the assumption of $U \geq R$ and $U_r \geq 1$. We thus use index k for indicating both RIS k and its associated UE so that k replaces r, u in (1) and (2).

Let $\mathcal{S} \subset \{1, \cdots, R\}$, $|\mathcal{S}| = K$ be the scheduler output, which consists of the selected RIS-UE pairs. Considering the ZFBF matrix $\mathbf{F} = [\mathbf{f}_1, \mathbf{f}_2, \cdots, \mathbf{f}_K]$ which is obtained by $\mathbf{F} = (\mathbf{H})^{\dagger}$, the RIS-based sum rate of the selected RIS-UE set \mathcal{S} is then obtained as in [14], [15] by

$$R(S) = \sum_{k=1}^{K} R_k = K \log_2 \left(1 + \frac{\rho_k}{\|F\|_F^2} \right),$$
(3)

where R_k is the individual rate for UE k, ρ_k indicates the received signal-to-noise ratio (SNR) at UE k. For theoretical analysis, we assume that the simple and practical case of uniform power allocation over all downlink streams where $\rho_k = \rho, \forall k \in \{1, \cdots, K\}$. Given this general RIS model, our goal is to derive the asymptotic distribution of the RIS-based sum rate and achievable scheduling gain.

III. Gaussian Approximation of the RIS-based Sum Rate

In this section, we analyze the asymptotic distribution of the RIS-based sum rate. In (3), the RIS-based sum rate depends only on $||F||_F^2$. Therefore, we can gain insight into

the distribution of the RIS-based sum rate by analyzing the distribution of $\|\mathbf{F}\|_{\mathrm{F}}^2$.

A. Analysis of the distribution of $\|\mathbf{F}\|_{\mathrm{F}}^2$

From (2), $\boldsymbol{h}_{\text{eff},k}^{\text{H}} = \boldsymbol{h}_{k}^{\text{H}} + \bar{\boldsymbol{h}}_{k}^{\text{H}}$ where $\bar{\boldsymbol{h}}_{k} = \sqrt{N}\boldsymbol{R}_{k}^{1/2}\boldsymbol{z}_{k}^{\text{H}}$ which is the indirect link between the BS and UE k through RIS k. Then, the aggregate downlink channel \boldsymbol{H} can be obtained by

$$\boldsymbol{H} = \left[\boldsymbol{h}_{\text{eff},1}^{\text{H}}, \cdots, \boldsymbol{h}_{\text{eff},K}^{\text{H}}\right]^{\text{T}}$$
$$= \left[\boldsymbol{h}_{1}^{\text{H}} + \bar{\boldsymbol{h}}_{1}^{\text{H}}, \cdots, \boldsymbol{h}_{K}^{\text{H}} + \bar{\boldsymbol{h}}_{K}^{\text{H}}\right]^{\text{T}} = \tilde{\boldsymbol{H}} + \bar{\boldsymbol{H}}, \quad (4)$$

where $\tilde{\boldsymbol{H}} = [\boldsymbol{h}_1^{\mathrm{H}}, \cdots, \boldsymbol{h}_K^{\mathrm{H}}]$ and $\bar{\boldsymbol{H}} = [\bar{\boldsymbol{h}}_1^{\mathrm{H}}, \cdots, \bar{\boldsymbol{h}}_K^{\mathrm{H}}]$ are aggregate direct and indirect channel matrices respectively. According to [15], $\|\boldsymbol{F}\|_{\mathrm{F}}^2 = \mathrm{tr}(\boldsymbol{A}^{-1})$, where $\boldsymbol{A} = \boldsymbol{H}\boldsymbol{H}^{\mathrm{H}}$. Therefore, $\|\boldsymbol{F}\|_{\mathrm{F}}^2$ can be approximated as

$$\|\boldsymbol{F}\|_{\mathrm{F}}^{2} = \operatorname{tr}(\boldsymbol{A}^{-1}) = \operatorname{tr}\left\{\left(\tilde{\boldsymbol{A}} + \bar{\boldsymbol{R}}\right)^{-1}\right\}$$

$$\stackrel{\text{(a)}}{\approx} \operatorname{tr}\left\{\left(\tilde{\boldsymbol{A}} + \bar{\boldsymbol{A}}\right)^{-1}\right\}$$

$$\stackrel{\text{(b)}}{=} \operatorname{tr}\left\{\tilde{\boldsymbol{A}}^{-1} - \frac{1}{1 + \operatorname{tr}(\bar{\boldsymbol{A}}\tilde{\boldsymbol{A}}^{-1})}\tilde{\boldsymbol{A}}^{-1}\bar{\boldsymbol{A}}\tilde{\boldsymbol{A}}^{-1}\right\}$$

$$\stackrel{\text{(c)}}{\approx} \operatorname{tr}(\tilde{\boldsymbol{A}}^{-1}) - \frac{\operatorname{tr}(\tilde{\boldsymbol{A}}^{-2})}{\operatorname{tr}(\tilde{\boldsymbol{A}}^{-1})},$$
(5)

where $\tilde{\pmb{A}} = \tilde{\pmb{H}}\tilde{\pmb{H}}^H$, $\bar{\pmb{A}} = \bar{\pmb{H}}\bar{\pmb{H}}^H$, and $\bar{\pmb{R}} = \bar{\pmb{H}}\bar{\pmb{H}}^H + \tilde{\pmb{H}}\bar{\pmb{H}}^H + \bar{\pmb{H}}\bar{\pmb{H}}^H + \bar{\pmb{H}}\bar{\pmb{H}}^H$, (a) results from the fact that the elements in $\bar{\pmb{A}}$ are are dominant values in $\bar{\pmb{R}}$ for large M, (b) is obtained by [16] since rank $(\bar{\pmb{A}}) = 1$, and (c) results from the assumption of large M. From [17] and [18], $\mathrm{Var}[\mathrm{tr}(\tilde{\pmb{A}}^{-1})]$ and $\mathrm{Var}[\mathrm{tr}(\tilde{\pmb{A}}^{-2})]$ will converge to 0 as M goes to infinity, and from [19], $\mathrm{E}[\mathrm{tr}(\tilde{\pmb{A}}^{-1})] = \beta$ and $\mathrm{E}[\mathrm{tr}(\tilde{\pmb{A}}^{-2})] = \frac{M\beta}{(M-K)^2-1}$ where $\beta = \frac{K}{M-K}$. Then, the expectation and variance of $\|\pmb{F}\|_{\mathrm{F}}^2$ can be obtained as follows:

$$E[\|\boldsymbol{F}\|_{F}^{2}] = E\left[\operatorname{tr}(\tilde{\boldsymbol{A}}^{-1})\right] - \frac{E\left[\operatorname{tr}(\tilde{\boldsymbol{A}}^{-2})\right]}{E\left[\operatorname{tr}(\tilde{\boldsymbol{A}}^{-1})\right]}$$
$$= \beta - \frac{M\beta^{2}}{K^{2} - \beta^{2}}, \tag{6}$$

$$\operatorname{Var}\left[\|\boldsymbol{F}\|_{\mathrm{F}}^{2}\right] = \operatorname{Var}\left[\operatorname{tr}(\tilde{\boldsymbol{A}}^{-1}) - \frac{\operatorname{tr}(\tilde{\boldsymbol{A}}^{-2})}{\operatorname{tr}(\tilde{\boldsymbol{A}}^{-1})}\right]$$

$$\stackrel{\text{(d)}}{\approx} \operatorname{Var}\left[\operatorname{tr}\left(\tilde{\boldsymbol{A}}^{-1}\right)\right] \stackrel{\text{(e)}}{=} \beta^{3}\left(\frac{\beta+1}{K^{2}-\beta^{2}}\right), \quad (7)$$

where (d) results from [17] and [18] for large M, and (e) results from [15] since \tilde{A} has only direct components between the BS and the UEs. Finally, from (6) and (7), the distribution of $||F||_F^2$ is obtained from the following lemma.

Lemma 1. $\|F\|_{\mathrm{F}}^2$ follows an i.i.d. Gaussian distribution as follows:

$$\|\mathbf{F}\|_{\mathrm{F}}^2 \stackrel{d}{\to} \mathcal{N}\left(\gamma, \beta^3 \left(\frac{\beta+1}{K^2-\beta^2}\right)\right)$$
 (8)

where $\gamma = \beta - \frac{M\beta^2}{K^2 - \beta^2}$ and $\stackrel{d}{\to}$ denotes a convergence in distribution

Proof. Let u_k be a user connected to RIS r_k . Since correlation matrix \mathbf{R}_{r_k} is defined as $\frac{1}{N}\mathbf{G}_{r_k}^H\mathbf{G}_{r_k}$, the entries of $\mathbf{h}_{\mathrm{eff},u_k}$ are independent random variables for different r_k . Since the aggregate downlink channel \mathbf{H} is composed of row vectors of $\mathbf{h}_{\mathrm{eff},u_k}$, $\|\mathbf{F}\|_{\mathrm{F}}^2$ follows an i.i.d. Gaussian distribution as proved in [20]. Using (6) and (7), $\|\mathbf{F}\|_{\mathrm{F}}^2$ follows an i.i.d. Gaussian distribution with mean γ and variance $\beta^3(\frac{\beta+1}{k^2-\beta^2})$.

B. Analysis of the distribution of RIS-based sum rate

From (3), the individual rate for user k will be:

$$R_{k} = \log_{2} \left(1 + \frac{\rho}{\|\mathbf{F}\|_{F}^{2}} \right)$$

$$= \underbrace{\log_{2} \left(\rho + \|\mathbf{F}\|_{F}^{2} \right)}_{R_{A}} - \underbrace{\log_{2} \left(\|\mathbf{F}\|_{F}^{2} \right)}_{R_{B}}.$$
(9)

From (6) and (7), $\|\mathbf{F}\|_{\mathrm{F}}^2$ converges to a deterministic value as K and M increase to infinity with M > K + 1:

$$\|\boldsymbol{F}\|_{\mathrm{F}}^2 \to \gamma$$
, as $K, M \to \infty$. (10)

 $R_{\rm A}$ in (9) can then be expressed as

$$R_{A} = \log_{2} \left(\frac{\rho + \|\boldsymbol{F}\|_{F}^{2}}{\rho + \gamma} \right) + \log_{2} \left(\rho + \gamma \right)$$

$$= \log_{2} \left(1 + \frac{\|\boldsymbol{F}\|_{F}^{2} - \gamma}{\rho + \gamma} \right) + \log_{2} \left(\rho + \gamma \right)$$

$$= \left(\|\boldsymbol{F}\|_{F}^{2} - \gamma \right) \log_{2} \left(1 + \frac{\|\boldsymbol{F}\|_{F}^{2} - \gamma}{\rho + \gamma} \right)^{\frac{1}{\|\boldsymbol{F}\|_{F}^{2} - \gamma}}$$

$$+ \log_{2} \left(\rho + \gamma \right). \tag{11}$$

From (10), $\|\mathbf{F}\|_{\mathrm{F}}^2 - \gamma$ converges to zero as K and M increase. Therefore, for large K and M, (11) can be approximated as

$$R_{\mathcal{A}} \stackrel{\text{(f)}}{\approx} \left(\|\boldsymbol{F}\|_{\mathcal{F}}^{2} - \gamma \right) \log_{2} e^{\frac{1}{\rho + \gamma}} + \log_{2}(\rho + \gamma)$$

$$= \frac{1}{\ln 2} \left(\frac{\|\boldsymbol{F}\|_{\mathcal{F}}^{2} - \gamma}{\rho + \gamma} \right) + \log_{2}(\rho + \gamma), \qquad (12)$$

where (f) results from the exponential function definition $e^x = \lim_{n\to\infty} (1+x/n)^n$. $R_{\rm B}$ in (9) can also be expressed as:

$$R_{\rm B} = \log_2 \left(\frac{\|\boldsymbol{F}\|_{\rm F}^2}{\gamma} \right) + \log_2 \gamma$$

$$\stackrel{\text{(g)}}{\approx} \left(\|\boldsymbol{F}\|_{\rm F}^2 - \gamma \right) \log_2 e^{\frac{1}{\gamma}} + \log_2 \gamma$$

$$= \frac{1}{\ln 2} \left(\frac{\|\boldsymbol{F}\|_{\rm F}^2 - \gamma}{\gamma} \right) + \log_2 \gamma, \tag{13}$$

where (g) also results from the exponential function definition for large K and M. From (12) and (13), the RIS-based individual rate for the UE k will be:

$$R_k = R_{\rm A} - R_{\rm B} = \frac{\rho}{\ln 2} \left(\frac{\gamma - \|\mathbf{F}\|_{\rm F}^2}{\gamma(\rho + \gamma)} \right) + \log_2 \left(1 + \frac{\rho}{\gamma} \right). \tag{14}$$

The RIS-based sum rate, R_{RIS} , can then be obtained as

$$R_{\text{RIS}} = \sum_{k=1}^{K} R_k = \frac{K\rho}{\ln 2} \left(\frac{\gamma - \|\mathbf{F}\|_{\text{F}}^2}{\gamma(\rho + \gamma)} \right) + K \log_2 \left(1 + \frac{\rho}{\gamma} \right).$$
(15)

From (14) and (15), it is observed that the distributions of both the individual and sum rates follow the distribution of $\|\mathbf{F}\|_{\mathrm{F}}^2$. According to Lemma 1, the RIS-based rates R_k and R_{RIS} follow i.i.d. Gaussian distributions.

The results of this section give us two insights. First, as shown in (15), the RIS-based sum rate is determined irrespective of the number of RIS elements N. This result is intuitive under our assumption of a system that has a very larger number of RISs and UEs, and where each RIS has a finite number of reflecting elements. Second, in comparison with the results from non-RIS systems [15], the ergodic sum rate of an RIS-based system is $K \log_2{(1+\rho/\gamma)}$ whereas the one of non-RIS system is $K \log_2{(1+\rho/\beta)}$. Under the condition of M > K+1 as in (10), γ is always smaller than β . This implies that adding RISs in a traditional MIMO system can improve the sum rate under certain conditions. Using the RIS-based sum rate, we next analyze the achievable sum rate and multiuser scheduling gain.

IV. ANALYSIS OF THE ACHIEVABLE SCHEDULING GAIN

The achievable sum rate is calculated by comparing every possible choice of the RIS-UE set S by [11]

$$R_{\max} = \max_{\mathcal{S} \subset \{1, \dots, R\}, |\mathcal{S}| \le M} R(\mathcal{S}) = \max_{1 \le K \le M} \overline{R}_K(\mathcal{S}), \quad (16)$$

where $\overline{R}_K(\mathcal{S})$ is achievable sum rate for K RIS-UE pairs given by

$$\overline{R}_K(\mathcal{S}) = \max_{\mathcal{S} \subset \{1, \dots, R\}: |\mathcal{S}| = K} R(\mathcal{S}) = \max_{\mathcal{S} \subset \{1, \dots, R\}} R_K(\mathcal{S}),$$
(17)

where $R_K(\mathcal{S})$ is essentially $R(\mathcal{S})$ with $|\mathcal{S}| = K$. To obtain $\overline{R}_K(\mathcal{S})$, an exhaustive search over the entire space of RIS-UE pair sets for that value of K is required. Such an exhaustive search based scheduler compares $\binom{R}{K}$ UE sets and determines the RIS-UE pair set maximizing the sum rate; $\binom{R}{K}$ denotes the K-combinations of a set with R elements. Assuming a very large R, it is impossible to obtain $\overline{R}_K(\mathcal{S})$ by exhaustive search, because of the associated computational complexity. In the following subsections, we asymptotically obtain $\overline{R}_K(\mathcal{S})$ as well as the achievable scheduling gain.

A. Asymptotic distribution of $R_K(S)$

Let us consider the possible RIS-UE pair sets $\mathcal{S}_k \subset \{1,2,\cdots,R\}: |\mathcal{S}_k| = K \text{ for } 1 \leq k \leq {R \choose K}, \text{ and a discrete random variable } R_K(\mathcal{S}) \text{ distributed over entire RIS-UE pair sets } \mathcal{S}_k.$ In this case, even if $\mathbf{h}_{\text{eff},1},\cdots,\mathbf{h}_{\text{eff},U}$ are independent random vectors, the aggregate downlink channel matrices of arbitrarily chosen RIS-UE pair sets, $\mathbf{H}(\mathcal{S}_k)$, may include partially overlapping elements in several \mathcal{S}_k . However, the following lemma proves that the proportion of partially

overlapping matrices $H(S_k)$ becomes zero when R goes to infinity with $R \gg K^2$.

Lemma 2. Let S_i be one of the possible RIS-UE pair sets $S_k \subset \{1, 2, \dots, R\} : |S_k| = K$ for $1 \le k \le {R \choose K}$, and S_j be a RIS-UE pair set arbitrarily selected from the sets S_k . As R goes to infinity with $R \gg K^2$, the probability of intersection between S_i and S_j almost surely converges to zero, i.e.,

$$\lim_{R \to \infty, R \gg K^2} \Pr(|S_i \cap S_j| \neq 0) = 0.$$

Proof. See Appendix A.

Lemma 2 states that, under the assumed conditions (R) increasing to infinity with $R\gg K^2$, the matrices $\boldsymbol{H}(\mathcal{S}_k)$ will not asymptotically include overlapping elements and, therefore, that they can be replaced by $\binom{R}{K}$ independent channel realizations. From (8) and [15], the distribution of achievable sum rates for independent channel realizations is obtained next.

Corollary 1. The achievable sum rates for independent channel realizations follow Gaussian distribution as $K, M \to \infty$ with M > K + 1, given by

$$R_{\rm RIS} \stackrel{d}{\to} \mathcal{N} \left(K \log_2 \left(1 + \frac{\rho}{\gamma} \right), \frac{\beta(\beta+1)}{K^2 - \beta^2} \left(\frac{K\rho}{(\rho+\beta) \ln 2} \right)^2 \right).$$
(18)

We next prove the following theorem.

Theorem 1. The RIS-based sum rate of K-user scheduling among R RIS-UE pairs, $R_K(\mathcal{S})$, approaches a continuous Gaussian distribution $R_{\rm RIS}$ when $R, M, K \to \infty$ with $R \gg K^2$ and $M > K+1: R_K(\mathcal{S}) \stackrel{d}{\to} R_{\rm RIS}$.

Proof. From Lemma 2, $R_K(\mathcal{S})$ becomes a discrete random variable generated by the sum rates of independent $\binom{R}{K}$ channel realizations. Moreover, $R_K(\mathcal{S})$ becomes a continuous random variable R_K , given that $\binom{R}{K}$ becomes infinite value as R goes to infinity. The asymptotic distribution of the sum rates for independent channel realizations of H has already been derived in Corollary 1. Therefore, R_{RIS} from Corollary 1 and R_K are identically distributed for very large $R \gg K^2$.

Theorem 1 states that the achievable RIS-based sum rate follows an i.i.d. Gaussian distribution. Using the characteristics of Gaussian distribution, we can obtain the achievable scheduling gain.

B. Asymptotic \overline{R}_K and achievable scheduling gain

The asymptotical achievable scheduling gain of R_K can be obtained by using the characteristics of the Gaussian distribution presented in Theorem 1. Based on the characteristics of the Gaussian distribution of R_K , we will use the following lemma on the maximum value of a sequence of independent Gaussian random variables [21].

Lemma 3. Let X_1, \ldots, X_p be a sequence of independent Gaussian random variables with mean μ and variance σ^2 .

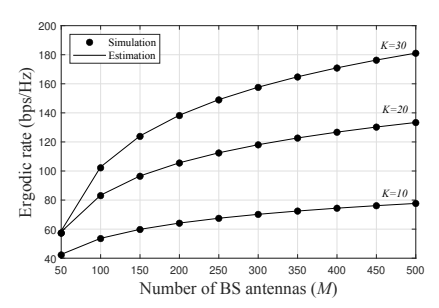


Fig. 2. Ergodic rates of a RIS-based system as a function of the number of BS antennas.

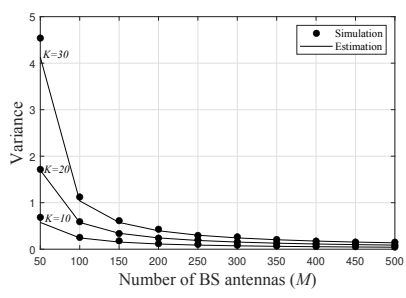


Fig. 3. Variances of downlink rates a RIS-based system as a function of the number of BS antennas.

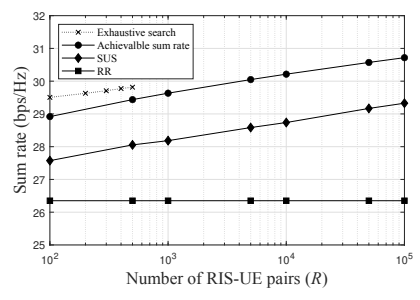


Fig. 4. Performance comparison of the RIS-based sum rates as a function of the number of RIS-UE pairs when M=64 and K=5.

Define $X_{\max}=\max(X_1,\ldots,X_p)$. Then $\frac{X_{\max}-\mu}{\sqrt{2\sigma^2\ln p}}\to 1$ as $p\to\infty$ in probability.

This lemma states that the maximum value in a sequence of independent Gaussian random variables converges to $\mu + \sqrt{2\sigma^2 \ln p}$ as p, the number of elements in the sequence, increases to infinity. We now note that \overline{R}_K is the maximum value among the $\binom{R}{K}$ independent Gaussian random variables R_K , and that $\binom{R}{K}$ increases to infinity with R. Therefore, we can obtain the asymptotic \overline{R}_K by using both Theorem 1 and Lemma 3, as follows:

$$\overline{R}_K \approx K \log_2 \left(1 + \frac{\rho}{\gamma} \right) + \sqrt{2 \left(\frac{\beta(\beta+1)}{K^2 - \beta^2} \right) \left(\frac{K\rho}{(\rho+\beta) \ln 2} \right)^2 \ln \binom{R}{K}}. \quad (19)$$

We finally derive the achievable scheduling gain α_K from the last term in (19). For a more intuitive analysis of the achievable scheduling gain, we simplify α_K as follows:

$$\alpha_K \stackrel{\text{(h)}}{\approx} \frac{K\rho}{\left(\rho + \frac{K}{M - K}\right)\ln 2} \sqrt{\frac{2M}{(M - K)^2 - 1} \left\{1 + \ln \frac{R}{K}\right\}},$$
(20)

where (h) results from using the following approximation for $\binom{R}{K}$ as R goes to infinity with $R \gg K^2$:

$$\ln \binom{R}{K} \stackrel{\text{(i)}}{\approx} R \ln R - K \ln K - (R - K) \ln(R - K) \quad (21)$$

$$\stackrel{\text{(j)}}{\approx} K + K \ln \left(\frac{R}{K}\right), \quad (22)$$

where (i) results form the Stirling's approximation $\ln n! \approx n \ln n - n$ [22] and (j) is obtained by the definition of the exponential function $e^x = \lim_{n \to \infty} (1 + x/n)^n$.

The channel hardening effect can be observed in terms of multiuser scheduling by considering the achievable scheduling gain α_K in (20). When R, M and K increase to infinity under the condition $R\gg K^2$, α_K follows an $O\left(\sqrt{M\log R}\right)$ law, and \overline{R}_K increase as $O\left(M+\sqrt{M\log R}\right)$. In these conditions, we observe:

1) For $R=M^c$: \overline{R}_K follows an O(M) law, and the achievable scheduling gain vanishes. In this case, channel hardening effect occurs.

2) For $R = \exp(M)$: Both α_K and \overline{R}_K follow an O(M) law. However, the achievable scheduling gain does not vanish. Therefore, the reduced channel hardening effect occurs.

3) For $R = \exp(M^2)$: \overline{R}_K follows an $O(M\sqrt{M})$ law, and only achievable scheduling gain is preserved. In this case, there is no channel hardening effect.

In conclusion, the occurrence of the channel hardening effect strongly depends on the relationship between R and M and its impact on $O\left(M + \sqrt{M \log R}\right)$.

V. SIMULATION RESULTS

We assess our results using extensive simulations. We evaluate the accuracy of Theorem 1 by comparing the asymptotic results with the simulated results in terms of the ergodic rate and variance of $R_{\rm RIS}$. In the subsequent figures, the label "Estimation" refers to the results obtained from Theorem 1 whereas the label "Simulation" refers to the results obtained from the Monte Carlo simulation. We also compare our results with two representative multiuser scheduling algorithms; semiorthogonal user selection (SUS) [11], and round robin (RR). In SUS, the node having maximum orthogonality with previously selected nodes is successively selected whereas the UEs are fairly selected without the scheduling gain in RR. In the simulations, the transmit SNR is assumed to be 6 dB.

Figs. 2 and 3 show the ergodic rates and the variance of the simulation and the estimation from Theorem 1 as M increases and K varies from 10 to 30. Clearly, the results from the estimation closely match the simulation results over the entire range of M and K. From Fig. 2, we observe that the ergodic rate increases with increasing M since γ decreases as M increases. We also observe that the ergodic rate almost proportionally increases as K increases. In Fig. 3, the variance of sum rate decreases as M increases due to the increasing impact of the channel hardening effect. On the other hand, we can observe the variance increases with K which means that we can get a higher scheduling gain with larger K.

Fig. 4 compares the achievable sum rate and the sum rates obtained from the exhaustive search, SUS, and RR schemes as a function of the number of RIS-UE pairs R with M=64 and K=5. The results of achievable sum rate include the estimation from the achievable scheduling gain (20). The achievable sum rate and the sum rate of SUS increase as R increases because of the increasing scheduling gain whereas

the sum rate of RR is unaffected by R. The exhaustive search scheme is shown only up to R=500 due to the computational complexity but we can observe that the achievable sum rate converges to the results from the exhaustive search as R increases. This complies the result we proved in Theorem 1 and Lemma 3. As R increases, the gap between the exhaustive search and the achievable sum rate will gradually decrease, and finally, they are expected to converge at the same performance for extremely large R. From Fig. 4 we can also observe that the achievable sum rate can be used as a sum rate upper bound to verify the scheduling algorithm performance.

VI. CONCLUSION

In this paper, we have investigated the achievable sum rate of multiuser scheduling in RIS-based massive MIMO systems. We have asymptotically analyzed the achievable gain of the RIS-based ergodic sum rate compared to the non-RIS system. In addition, we have derived that the RIS-based sum rate follows a Gaussian distribution with a certain mean and variance. Using the characteristics of the Gaussian distribution, we have shown that the achievable sum rate increases as $O(M + \sqrt{M \log R})$ whereas the achievable scheduling gain follows an $O(\sqrt{M \log R})$ law. As a result, we have shown that the occurrence of the channel hardening effect depends on the relationship between M and R. Numerical results obtained from the derived achievable sum rate are shown to closely match Monte Carlo simulations. Simulation results also show that the achievable sum rate constitutes a good performance bound to verify the various multiuser scheduling algorithms, as well as converges the exhaustive search bound in RIS-based massive MIMO systems.

APPENDIX A PROOF OF LEMMA 2

Proof. Let S_i be one of the possible RIS-UE pair sets $S_k \subset \{1, 2, \cdots, R\} : |S_k| = K$ for $1 \leq k \leq {R \choose K}$, and S_j be a RIS-UE pair set arbitrarily selected from among the sets S_k . The probability that S_i and S_j do not intersect is given by

$$\Pr\left(\left|S_{i} \cap S_{j}\right| = 0\right) = \frac{\binom{R-K}{K}}{\binom{R}{K}}.$$
(23)

Equation (23) can be approximated as follows:

$$\frac{\binom{R-K}{K}}{\binom{R}{K}} = \exp\left[\ln\left(\frac{\binom{R-K}{K}}{\binom{R}{K}}\right)\right] \stackrel{\text{(k)}}{\approx} \exp\left(-\frac{K^2}{R}\right),$$

where (k) results from (21) and the exponential function definition $e^x = \lim_{n \to \infty} (1 + x/n)^n$, under the assumption of a very large $R \gg K^2$. Therefore, as R increases to infinity with $R \gg K^2$, the probability that \mathcal{S}_j intersects any one of \mathcal{S}_i almost surely converges to zero, as follows:

$$\lim_{R \to \infty} \Pr(|S_i \cap S_j| \neq 0) = 1 - \lim_{R \to \infty} \exp\left(\frac{-K^2}{R}\right) = 0.$$

REFERENCES

- A. Nauman, Y. A. Qadri, M. Amjad, Y. B. Zikria, M. K. Afzal, and S. W. Kim, "Multimedia internet of things: A comprehensive survey," *IEEE Access*, vol. 8, pp. 8202–8250, 2020.
- [2] E. Basar, M. Di Renzo, J. De Rosny, M. Debbah, M.-S. Alouini, and R. Zhang, "Wireless communications through reconfigurable intelligent surfaces," *IEEE Access*, vol. 7, pp. 116753–116773, 2019.
- [3] S. Hu, F. Rusek, and O. Edfors, "Beyond massive MIMO: The potential of data transmission with large intelligent surfaces," *IEEE Trans. Signal Process.*, vol. 66, no. 10, pp. 2746–2758, May 2018.
- [4] N. S. Perović, L.-N. Tran, M. Di Renzo, and M. F. Flanagan, "Achievable rate optimization for MIMO systems with reconfigurable intelligent surfaces," *IEEE Trans. Wireless Commun.*, vol. 20, no. 6, pp. 3865– 3882, 2021.
- [5] C. Huang, A. Zappone, G. C. Alexandropoulos, M. Debbah, and C. Yuen, "Reconfigurable intelligent surfaces for energy efficiency in wireless communication," *IEEE Trans. Wireless Commun.*, vol. 18, no. 8, pp. 4157–4170, Aug. 2019.
- [6] S. Jia, X. Yuan, and Y.-C. Liang, "Reconfigurable intelligent surfaces for energy efficiency in D2D communication network," *IEEE Wireless Commun. Lett.*, vol. 10, no. 3, pp. 683–687, Mar. 2021.
- [7] P. Mursia, V. Sciancalepore, A. Garcia-Saavedra, L. Cottatellucci, X. C. Pérez, and D. Gesbert, "RISMA: Reconfigurable intelligent surfaces enabling beamforming for IoT massive access," *IEEE J. Sel. Areas Commun.*, vol. 39, no. 4, pp. 1072–1085, Apr. 2021.
- [8] L. Li, D. Ma, H. Ren, D. Wang, X. Tang, W. Liang, and T. Bai, "Enhanced reconfigurable intelligent surface assisted mmWave communication: A federated learning approach," *China Commun.*, vol. 17, no. 10, pp. 115–128, Oct. 2020.
- [9] M. Jung, W. Saad, M. Debbah, and C. S. Hong, "On the optimality of reconfigurable intelligent surfaces (RISs): Passive beamforming, modulation, and resource allocation," *IEEE Trans. Wireless Commun.*, vol. 20, no. 7, pp. 4347–4363, Jul. 2021.
- [10] M. Jung, W. Saad, Y. Jang, G. Kong, and S. Choi, "Performance analysis of large intelligent surfaces (LISs): Asymptotic data rate and channel hardening effects," *IEEE Trans. Wireless Commun.*, vol. 19, no. 3, pp. 2052–2065, 2020.
- [11] T. Yoo and A. Goldsmith, "On the optimality of multiantenna broad-cast scheduling using zero-forcing beamforming," *IEEE J. Sel. Areas Commun.*, vol. 24, no. 3, pp. 528–541, Mar. 2006.
- [12] Q.-U.-A. Nadeem, A. Chaaban, and M. Debbah, "Multi-user opportunistic beamforming using reconfigurable surfaces," arXiv, Dec. 2019. [Online]. Available: https://arxiv.org/abs/1912.07063
- [13] Q.-U.-A. Nadeem, A. Kammoun, A. Chaaban, M. Debbah, and M.-S. Alouini, "Asymptotic max-min SINR analysis of reconfigurable intelligent surface assisted MISO systems," *IEEE Trans. Wireless Commun.*, vol. 19, no. 12, pp. 7748–7764, Dec. 2020.
- [14] F. Rusek, D. Persson, B. K. Lau, E. G. Larsson, T. L. Marzetta, O. Edfors, and F. Tufvesson, "Scaling up MIMO: Opportunities and challenges with very large arrays," *IEEE Signal Process. Mag.*, vol. 30, no. 1, pp. 40–60, Jan. 2013.
- [15] M. Jung, T. Kim, K. Min, Y. Kim, J. Lee, and S. Choi, "Asymptotic distribution of system capacity in multiuser MIMO systems with large number of antennas," in *Proc. 2013 IEEE 77th Vehicular Technology Conference (VTC Spring)*, Dresden, Germany, 2013, pp. 1–5.
- [16] K. S. Miller, "On the inverse of the sum of matrices," *Mathematics Magazine*, vol. 54, no. 2, pp. 67–72, 1981.
- [17] J. Pielaszkiewicz and T. Holgersson, "Mixtures of traces of wishart and inverse wishart matrices," *Communications in Statistics - Theory and Methods*, vol. 50, no. 21, pp. 5084–5100, 2021.
- [18] P. Graczyk, G. Letac, and H. Massam, "The complex wishart distribution and the symmetric group," *The Annals of Statistics*, vol. 31, no. 1, pp. 287–309, Feb. 2003.
- [19] A. M. Tulino and S. Verdú, "Random matrix theory and wireless communications," *Foundations Trends Commun. Inf. Theory*, vol. 1, no. 1, pp. 1–182, Jun. 2004.
- [20] Q. Wu and R. Zhang, "Intelligent reflecting surface enhanced wireless network via joint active and passive beamforming," *IEEE Trans. Wireless Commun.*, vol. 18, no. 11, pp. 5394–5409, Nov. 2019.
- [21] R. Durrett, Probability: Theory and examples, 4th ed. Cambridge, U.K.: Cambridge Univ. Press, 2010.
- [22] M. Hazewinkel, Stirling Formula. Encyclopaedia of Mathematics. Springer, 2001.